The Three-Dimensional Distribution of Galactic AGB Stars with ALLWISE

Nicholas M. Hunt-Walker, Željko Ivezić, Andrew C. Becker

University of Washington, Department of Astronomy, Seattle, WA 98195

nmhw@uw.edu, ivezic@uw.edu, acbecker@uw.edu

1. Introduction

- brief intro to Gal structure

- SDSS and other recent results do not go into the plane

- mention a few studies that do (GLIMPSE etc) and ongoing data taking with DECam

- AGB stars: luminous in IR, relatively easy to find; mention MACHO and OGLE studies, refer to Jackson et al. IRAS-based study, lead to WISE

- brief description of WISE

- paper outline

The formation of galaxies like the Milky Way was long thought to be a steady process that created a smooth distribution of stars. This standard view was exemplified by the Bahcall & Soneira (1980) and Gilmore et al. (1989) models, described in detail by, e.g., Majewski (1993). It was further motivated by observations of other galaxies, as well as what little information was available from *High Precision Parallax Collecting Satellite* (*HIPPARCOS*, **?**) and smaller pencil-beam surveys. In these, the Milky Way is modeled by three discrete components described by simple analytic expressions: the thin disk, thick disk, and halo.

Review is **?**) (**?**)

The advent of the *Sloan Digital Sky Survey* (SDSS, York et al. 2000) alleviated these limitations, providing accurate digital multi-band optical photometry across a quarter of the sky, as well as the largest optical spectroscopic catalog thus far known. This new influx of data enabled the development and application of photometric parallax methods, using color-magnitude relations to estimate stellar distances. In turn, this led to the large scale "tomography" of the Milky Way via stellar distributions in the 7-dimensional space spanned by spatial coordinates (Jurić et al. 2008), velocity components (Bond et al. 2010), and metallicity (Ivezić et al. 2008). The resulting maps revealed rich, complex substructure in the distribution of the Milky Way's stars (e.g. Ivezić et al. 2000; Yanny et al. 2000; Vivas et al. 2001; Newberg et al. 2002; Majewski et al. 2003; Belokurov et al. 2006; Grillmair 2006; Vivas & Zinn 2006), deeply shaking the existing view of the Galaxy.

In order to move forward from where SDSS tomography left off, we require observations that span an area larger than that of SDSS with Galactic objects that can be seen through interstellar

dust out to large distances. Stars from the Asymptotic Giant Branch (AGB) are perfect candidates as probes to the Milky Way. AGB stars are represent the last stage of evolution for stars between 0.8 and 8 $M_{\odot}$ (Iben & Renzini 1983; Herwig 2005), so they are bound to reside throughout the galaxy wherever other stars are present. During this phase, they produce substantial stellar winds ($10^{-7} < \dot{M} < 10^{-4} M_{\odot}$ yr^{-1}, Olofsson et al. 2002) rich in SiO and amorphous carbon as they progress through being oxygen-rich to being carbon-rich. These winds collect into circumstellar shells that, when warmed by the stellar photosphere, shine brightly in the near- and mid-infrared (NIR & MIR respectively). ======= The structure of the Milky Way has for many years been uncertain, with historical models assuming three discrete components described by simple analytic expressions: the thin disk, thick disk, and halo (Bahcall & Soneira 1980; Gilmore et al. 1989; Majewski 1993). The advent of the *Sloan Digital Sky Survey* (SDSS, York et al. 2000) has since provided more detail, using accurate digital multi-band optical photometry across a quarter of the sky, as well as the largest optical spectroscopic catalog thus far known. These new data led to the large scale "tomography" of the Milky Way via stellar distributions in the 7-dimensional space spanned by spatial coordinates (Jurić et al. 2008), velocity components (Bond et al. 2010), and metallicity (Ivezić et al. 2008). The resulting maps revealed rich, complex substructure in the distribution of the Milky Way's stars (e.g. Ivezić et al. 2000; Yanny et al. 2000; Vivas et al. 2001; Newberg et al. 2002; Majewski et al. 2003; Belokurov et al. 2006; Grillmair 2006; Vivas & Zinn 2006), deeply shaking the existing view of the Galaxy.

In order to move forward from where SDSS tomography left off, we require observations that span an area larger than that of SDSS , with Galactic objects that can be seen through interstellar dust out to large distances. Stars from the Asymptotic Giant Branch (AGB) are perfect candidates to serve as these probes to the Milky Way. AGB stars represent the last stage of evolution for stars between 0.8 and 8 $M_{\odot}$ (Iben & Renzini 1983; Herwig 2005) – the mass-range with the highest number of stars as inferred from the Kroupa (2001) initial mass function that can also reach the final stages of stellar evolution within a galactic timescale. Because of this, they are bound to reside throughout the galaxy wherever other stars are present. This phase of evolution is marked by two distinct periods: the early AGB (E-AGB) and the thermally-pulsing AGB phases. During the latter of the two, AGB stars produce substantial dust-driven stellar winds ($10^{-7} < \dot{M} < 10^{-4}$ $M_{\odot}$ yr^{-1}, Olofsson et al. 2002) rich in oxides (SiO, Al_2O_3, etc.) and carbon-rich molecules (SiC, AmC, etc.), with the chemical dominance being highly dependent upon the metallicity of the host galaxy (Matsuura et al. 2005). Galaxies such as the Milky Way are expected to have a substantial population of oxygen-rich AGB stars (Habing et al. 1985), whereas low-metallicity galaxies such as the Magellanic clouds have been shown to possess AGB populations dominated by carbon-rich stars (Boyer et al. 2011). In both cases, the other species of AGB star is rarely seen, as richness in one chemical type (e.g. oxides) necessitates the almost complete capture of the other chemical type (e.g. carbon) in CO (Iben & Renzini 1983). Over time, these chemically-rich winds create vast circumstellar shells that, when warmed by the stellar photosphere, emit in the near- and mid-infrared (NIR & MIR respectively). Although the molecular species present in oxygen- and carbon-rich winds are vastly different, emission from both types produce strong IR emission near

10μm, visible out to the Magellanic clouds (Ishihara et al. 2011) and beyond. Thus, if these stars can be pinpointed by a survey with a wide area of observation and high positional accuracy, they can be used as markers for a map of the Milky Way (Tu & Wang 2013).

Such a survey can be found in the *Wide-field Infrared Survey Explorer* (WISE, Wright et al. 2010; Cutri et al. 2012), a space-based observatory that has imaged the entire sky in the MIR (3.4, 4.6, 12, and 22μm). Additionally, WISE has been positionally matched to the Two-Micron All-Sky Survey (2MASS), a four-year mission characterizing the full sky in the NIR. Thus, the WISE catalog presents with hundreds of millions of sources with photometry of unprecedented sensitivity and positional accuracy in the NIR and MIR–ideal for capturing AGB stars at Galactic distances. In this paper, we use samples of known Galactic and Magellanic AGB stars to formulate color-color criteria with WISE and 2MASS photometry that can produce a reliable catalog of IR AGB candidates. We then use these candidates in conjunction with estimates of Galactic dust extinction along the line of sight to produce a Galaxy-wide number density distribution of AGB stars.

In Section 2, we describe in detail the data that we use for our study. In Section 3, we describe the color-color criteria used to isolate AGB stars in the WISE dataset, and the color-magnitude relationships that were derived for these stars from the Large Magellanic Cloud and the Milky Way bulge. In Section 4, we describe the spatial density distribution of AGB candidates in the Milky Way. Our conclusions can be found in section 5.

2. Data Sources and Reduction

2.1. Data Sources

In this study, we rely heavily on data from the ALLWISE extension of the WISE survey, combining data from the initial All-Sky Data Release, the 3-band cryogenic data release, and the NEOWISE post-cryogenic data release (Cutri et al. 2013). The initial WISE All-Sky Data Release observed the sky between January and August 2010, observing the sky 1.2 times with four detectors, operating at 3.4, 4.6, 12, and 22μm. Hereon we refer to ALLWISE photometric bands at [3.4μm/4.6μm/12μm/22μm] as [$W1/W2/W3/W4$]. The positions of objects in the WISE catalog were calibrated to the 2MASS point source catalog. The 3-band cryogenic data release contains data from $W1$, 2, and 3, and surveyed 30% of the sky between August and October 2010. During the 3-band cryogenic survey, $W1$ and $W2$ operated with nearly the same sensitivity as during the full survey. Warming of the telescope reduced sensitivity in $W3$ and fully saturated $W4$. The NEOWISE post-cryogenic data release contains $W1$ and $W2$ measurements, with sensitivities close to those obtained during the full cryogenic phase. During this phase, WISE surveyed 70% of the sky. Data products from the post-cryogenic release included updated instrumental, astrometric, and photometric calibrations and reduction algorithms, resulting in much lower SNR. The overall number of sources compiled into ALLWISE totals over 747.6 million.

In order to generate a reliable, high-confidence catalog of Galactic candidate AGB stars, we must first define color-color criteria from known AGB star samples. We select AGB stars from three source catalogs: the *Optical Gravitational Lens Experiment-III Variable Star Catalog* (OGLE-III, Udalski et al. 2008; Soszyński et al. 2009, 2011), the *MAssive Compact Halo Objects* project (MACHO, Alcock et al. 1997), and the SIMBAD Astronomical Database (Wenger et al. 2000).

OGLE-III photometry for Long-Period Variables (LPVs) in the Small and Large Magellanic Clouds (SMC and LMC respsectively) was obtained between July 2001 and May 2009, with stars in the central 4.5-deg^2 of the LMC and SMC having an additional 5 observing seasons of photometry from OGLE-II. LPVs were classified into 3 categories: OGLE-III Small Amplitude Red Giants (OSARGs), Semi-Regular Variables (SRVs), and Miras. All AGB stars O-rich and C-rich AGB stars in OGLE-III were photometrically selected using reddening-free Wesenheit magnitudes, described in detail in Soszyński et al. (2009, 2011). [Describe the selection bit in a little more detail, along with their sample completeness, selection biases, and contamination fractions] Data reduction techniques are described in Udalski et al. (2008). The resulting samples yield 46,467 AGB stars from the LMC (37,203 O-rich; 9,264 C-rich) and 6,509 stars from the SMC (3,727 O-rich; 2,782 C-rich).

From MACHO we obtain the sample of SMC, LMC, and Galactic Bulge AGB stars used in Fraser et al. (2008) (14,861 stars). Why were these objects selected? Howe were they selected? What is their completeness, selection bias, and contamination fraction? Following Fraser et al. (2008), the objects are divided into sequences (seq) 1-4. Sequence 1 primarily contains Mira variables pulsating in their fundamental modes, whereas Sequences 2-4 contain semi-regular variables in various pulsation modes.

The sample of AGB stars from SIMBAD was obtained by querying all objects classified as C-stars (18,656), S-stars (1,108), OH/IR stars (825), AGB stars (2,359), and Mira variables (9,608), for a total of 32,556 stars. Objects are classified spectroscopically, though by a variety of methods owing to the heterogeneous data housed within SIMBAD. Together with MACHO and OGLE-III, the total sample of AGB stars is 100,393. Because there is a high likelihood that samples between OGLE-III, MACHO, and SIMBADoverlap, we retain only unique objects after the initial data reduction in section 2.2.

We use SDSS spectroscopic catalogs to find and quantify regions in NIR-MIR color-color space populated by plausible contaminant sources. These include any Galactic stellar objects and planetary nebulae, as well as a host of extragalactic sources. Data for active galactic nuclei (AGN; 19,184 objects), quasi-stellar objects (QSOs; 122,550 objects), and star forming/burst galaxies (820,272 objects total) were drawn from SDSS DR7, specifically from the NYU Value Added Galaxy Catalog[1] (Blanton et al. 2005, VAGC). Luminous Red Galaxies (LRGs) were selected from the SDSS Luminous Red Galaxy Survey (105,631 objects, Kazin et al. 2010). Data for stars in the SDSS stellar locus were drawn from the DR 9 SEGUE Stellar Parameters Pipeline (SSPP)

[1] http://sdss.physics.nyu.edu/vagc/

(1,843,190 objects, Ahn et al. 2012). Include bit about YSOs and PNe from SIMBAD

2.2. Data Reduction

We use NASA/IPAC IRSA's GATOR tool[2] to positionally match SDSS, OGLE-III, MACHO, and SIMBAD to ALLWISE. We select only matches within 3" between each sample and ALLWISE. All samples of AGB were required to be brighter than the published 5σ faint limits of [16.83/15.6/11.32/8.0], as well as fainter than the saturation limits of [2.0/1.5/-3.0/-4.0] extrapolated from the wings of the PSFs for point sources, for $[W1/W2/W3/W4]$ (Cutri et al. 2013), with no flags for confusion or contamination as a spurious source in any band. We also require only single associations with 2MASS objects within 3", detections in $[J/K_S/W1/W2/W3/W4]$, and SNR > 3 in each ALLWISE band.

The population for each sample from initial matching as well as after the application of the ALLWISE faint limits, saturation limits, and 2MASS detection requirements are shown in Table 1. The WISE color-color distributions for the AGB and contaminant samples are shown in Figure 1.

Population	SIMBAD AGB*	C*	Mira	OH/IR	S*
3" match	1,689	14,209	9,027	406	1,081
Reduced	684	1,782	3,241	43	511
Population	MACHO seq1	seq2	seq3	seq4	
3" match	5,279	3,519	2,619	3,070	
Reduced	277	185	73	61	
Population	OGLE-III C-rich	O-rich			
3" match	11,542	38,848			
Reduced	249	730			
Population	DR12 SSPP	DR7 LRG	QSO	AGN	Galaxies
3" match	1,578,329	104,345	103,590	18,528	841,712
Reduced	67,508	84	3,977	1,069	44,314

Table 1: AGB and contaminant populations matched to WISE before and after sample reduction in section 2.2. MACHO sequences (seq1-seq4) are from Fraser et al. (2008) and described briefly in section 2.1.

3. Object Selection Criteria

In creating color-color criteria to generate a catalog of AGB candidates, we seek to maximize AGB completeness while minimizing contamination from non-AGB objects to beneath the 1% level.

[2] http://irsa.ipac.caltech.edu/cgi-bin/Gator/nph-scan?mission=irsa&submit=Select&projshort=WISE

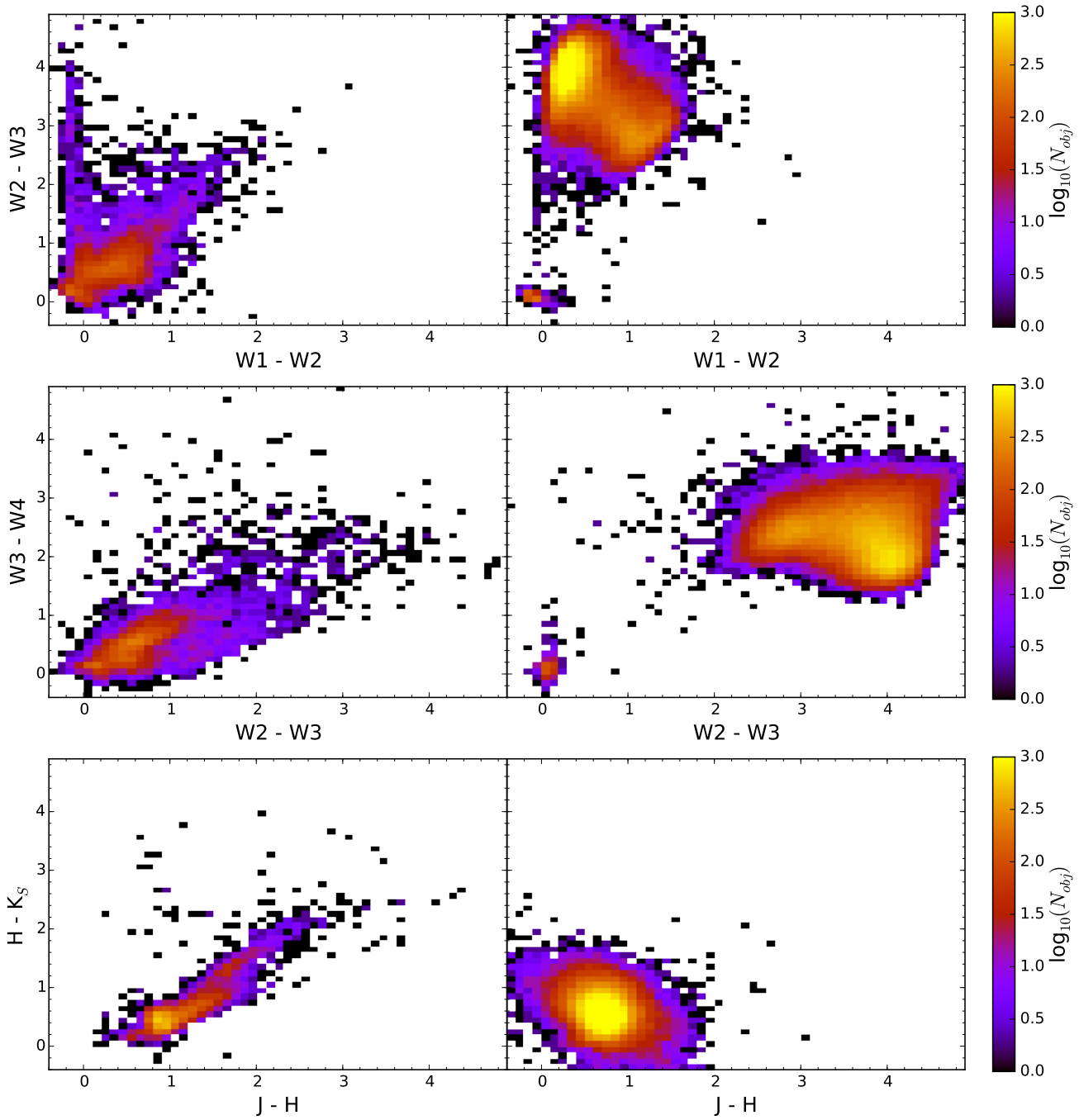

Fig. 1.— Logarithmic number densities for objects in WISE and 2MASS color-color space, binned in 0.1 dex on each axis. *Left:* The combined AGB sample matched to ALLWISE. *Right:* The combined contaminant sample.

The color-color criteria for AGB selection are as follows:

$$(J - K_s) > 1.1 \quad (1)$$

$$(W2 - W3) > 0.3 \quad (2)$$

$$(W3 - W4) < -0.83(W2 - W3) + 3.37 \quad (3)$$

The criteria in (1) and (2) are primarily concerned with rejecting objects from the stellar locus, and other objects whose NIR spectra are dominated by the Rayleigh-Jeans tail. (3) also rejects stars from the stellar locus, but primarily functions to remove IR-bright extragalactic sources.

We also experiment with other criteria to focus more closely on the high-reliability AGB population, instead of trying to capture the most AGB-like objects. These criteria are as follows:

$$(W1 - W2) < 1 \quad (4)$$

$$(W2 - W3) < 1 \quad (5)$$

Criteria (**??**) restricts NIR excesses. Criteria (5) primarily removes extragalactic sources, while only slightly cutting into the distribution of known AGB stars.

Sample completeness η is defined as

$$\eta = \frac{N - n_{\rm missed}}{N}$$

where N is the total number of objects in the sample, and $n_{\rm missed}$ is the number of objects outside of the applied boundaries. Figure 2 shows the distribution of sample completeness amongst AGB sources after the application of the above criteria. The vast majority (79.07%) of Galactic AGB stars is recovered after criteria (1), (2), and (3) are applied. The largest losses occur at the edges of the Galactic disk ($|b| \approx 10°$) and in regions of high stellar number density both in the Galaxy and the Magellanic Clouds. In the color-color diagrams, selection completeness degrades near the borders of the selection area, as objects that straddle these boundaries may exhibit enough emission in other color-color spaces to be removed by our criteria. Of the remaining sample of 5,709 objects, 52.94% lie within the disk ($|b| < 10°$).

Ivezić et al. (2013) defines sample contamination as

$$\epsilon = \frac{n_{\rm spurious}}{n_{\rm selected}}.$$

where $n_{\rm spurious}$ is the number of spurious sources and $n_{\rm selected} = N + n_{\rm spurious}$. The contamination map is shown in Figure 3. Most bins in Figure 3 exhibit 0% contamination, with the overall contamination level at 0.38%. What contaminants do remain exist primarily at the very fringes of the AGB star distribution in $(J - K_S)$ vs $(W2 - W3)$ space and near the redder boundary in $(W3 - W4)$ vs $(W2 - W3)$, where bluer extragalactic sources creep into the selection region. The results of the applied criteria on both the collective AGB and contaminant samples are summarized in Table 3.

Table 2: Samples Recovered wih Application of Criteria (%)

Object Type	Reduced	(1)	(2)	(3)	(1,2)	(1,2,3)	—	**(4)**	**(5)**	**(1,2,4)**	**(1,2,5)**	**(1,2,4,5)**
All AGBs	7220	95.15	84.89	95.21	82.62	79.07	—	**94.22**	**88.82**	**77.05**	**72.71**	**71.14**
O-rich AGB	3147	98.98	100.00	100.00	98.98	98.98	—	**98.44**	**97.33**	**97.43**	**96.31**	**94.88**
C-rich AGB	540	99.26	99.81	99.26	99.07	98.33	—	**57.59**	**63.33**	**56.85**	**62.59**	**54.44**
Unclassed AGB	3533	91.11	69.15	90.32	65.53	58.39	—	**96.07**	**85.14**	**61.99**	**53.24**	**52.53**
DR12 SSPP	67508	76.16	99.16	0.91	76.07	0.05	—	**86.05**	**0.89**	**65.67**	**0.03**	**0.03**
DR7 LRG	84	96.43	100.00	0.00	96.43	0.00	—	**89.29**	**0.00**	**85.71**	**0.00**	**0.00**
QSO	3783	73.54	99.97	0.13	73.54	0.11	—	**34.50**	**0.11**	**27.54**	**0.08**	**0.08**
Galaxy	42066	78.55	100.00	0.01	78.54	0.00	—	**96.39**	**0.01**	**75.31**	**0.00**	**0.00**
AGN	1011	79.33	100.00	0.00	79.33	0.00	—	**96.34**	**0.00**	**75.87**	**0.00**	**0.00**

We note that while we do achieve a low rate of contamination, most of our contaminant sources are out of the plane of the Galaxy, while many of our AGB sources are within the Galactic disk. Considering how our extragalactic contaminant sources are from various iterations of SDSS, we know that their spatial distributions should be effectively uniform across the sky [cite me]. For contaminants unaffected by interstellar reddening, they would occupy the same regions of color-color space already marked by our existing contaminant sample, and would similarly be removed by (1), (2), and (3). This would produce the same zero-level contamination for all extragalactic sources aside from QSOs. We can adopt a QSO spatial density by dividing the total number of spectroscopically identified QSOs by the covered area on the sky. Using this, we recover a QSO spatial density of some number per square degree. Using that density, and assuming ubiquity of sources on the sky, complete detection of QSOs down to some magnitude limit, and a lack of interstellar reddening, we can estimate a maximum QSO contamination fraction of some number. We use this number to report our QSO contamination fraction in Table 3, as QSOs significantly affected by interstellar reddening would exist further outside of the limits of (1), (2), and (3). A more rigorous study of QSO spatial density is outside the scope of this paper.

The remaining contaminant sample is from the SDSS DR12 SSPP, with the number of remaining species found within shown in Figure 4. the figures don't match up with each other. The number of red stars on the right side of the fig are significantly less than those in the histogram. Reconcile this.

4. AGB Candidate Distribution

Put words here

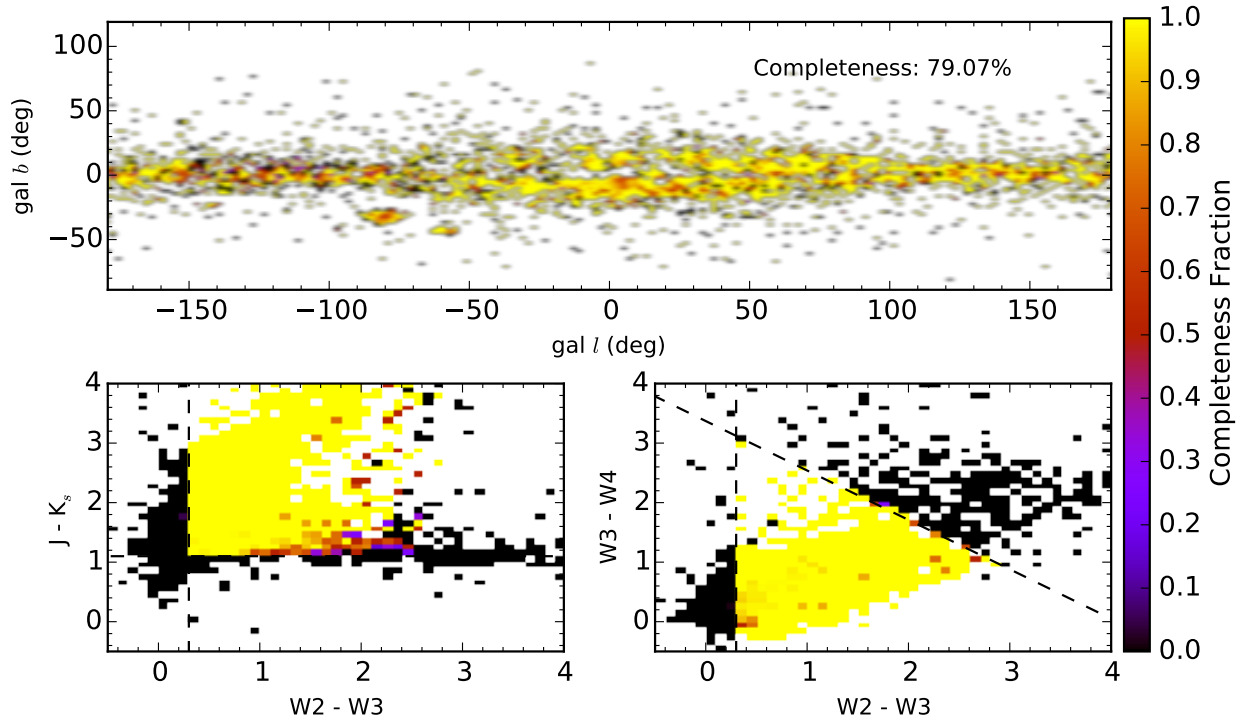

Fig. 2.— Sample selection completeness maps in (l, b) space (*top*) and the color-color space of our selection criteria (*bottom*). Color scale shows the completeness fraction per bin, with 4-deg^2 bins on the Galactic map and 0.1 dex bins on each axis of the color-color diagrams. Selection criteria are shown as dashed lines.

5. Conclusions

Put words here

REFERENCES

Ahn, C. P., et al. 2012, *Ap. J. Suppl.*, 203, 21

Alcock, C., et al. 1997, *Ap. J.*, 482, 89

Bahcall, J. N., & Soneira, R. M. 1980, *Ap. J. Suppl.*, 44, 73

Belokurov, V., et al. 2006, *Ap. J. (Letters)*, 642, L137

Blanton, M. R., et al. 2005, *A. J.*, 129, 2562

Bond, N. A., et al. 2010, *Ap. J.*, 716, 1

Boyer, M. L., et al. 2011, *A. J.*, 142, 103

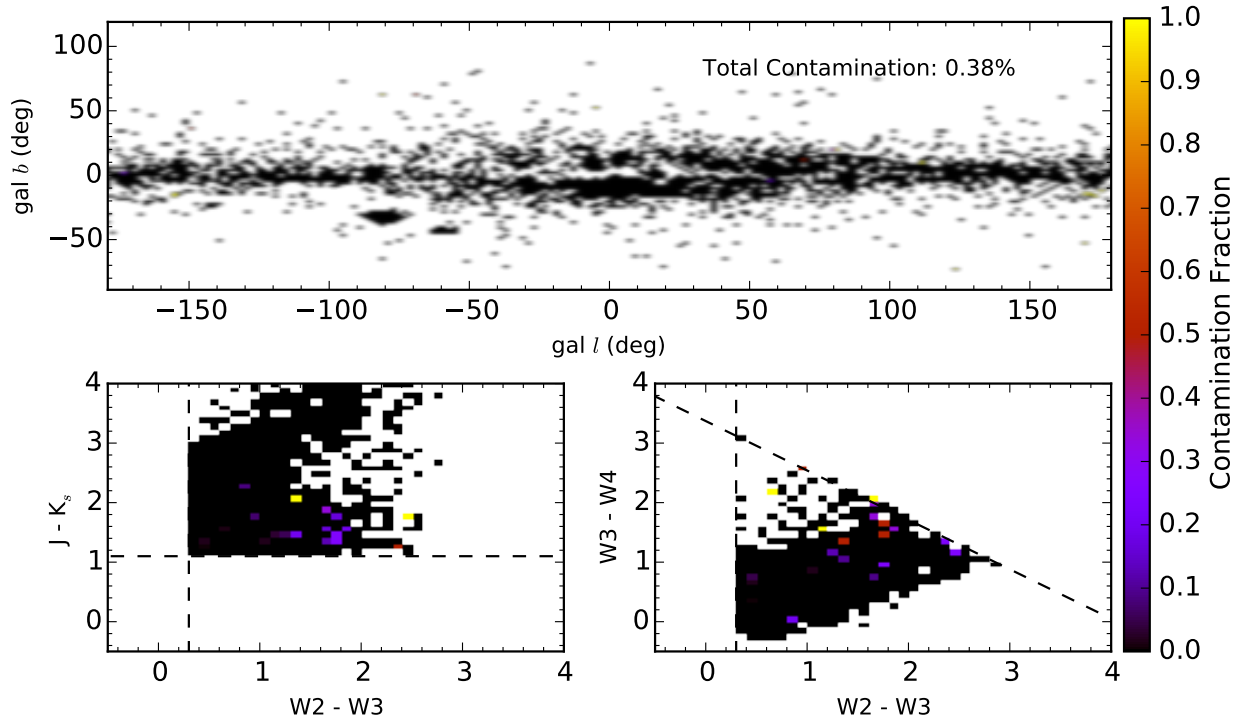

Fig. 3.— Sample contamination in Galactic (l, b) space (*top*) and color-color space (*bottom*). Boundaries and binning the same as Fig 2.

Cutri, R. M., et al. 2012, Explanatory Supplement to the WISE All-Sky Data Release Products, Tech. rep.

—. 2013, Explanatory Supplement to the AllWISE Data Release Products, Tech. rep.

Fraser, O. J., Hawley, S. L., & Cook, K. H. 2008, *A. J.*, 136, 1242

Gilmore, G., Wyse, R. F. G., & Kuijken, K. 1989, *Ann. Rev. Astr. Ap.*, 27, 555

Grillmair, C. J. 2006, *Ap. J. (Letters)*, 651, L29

Habing, H. J., Olnon, F. M., Chester, T., Gillett, F., & Rowan-Robinson, M. 1985, *Astr. Ap.*, 152, L1

Herwig, F. 2005, *Ann. Rev. Astr. Ap.*, 43, 435

Iben, Jr., I., & Renzini, A. 1983, *Ann. Rev. Astr. Ap.*, 21, 271

Ivezić, Ž., Beers, T. C. & Jurić, M. 2012, ARA&A, 50, 251

Ishihara, D., Kaneda, H., Onaka, T., Ita, Y., Matsuura, M., & Matsunaga, N. 2011, *Astr. Ap.*, 534, A79

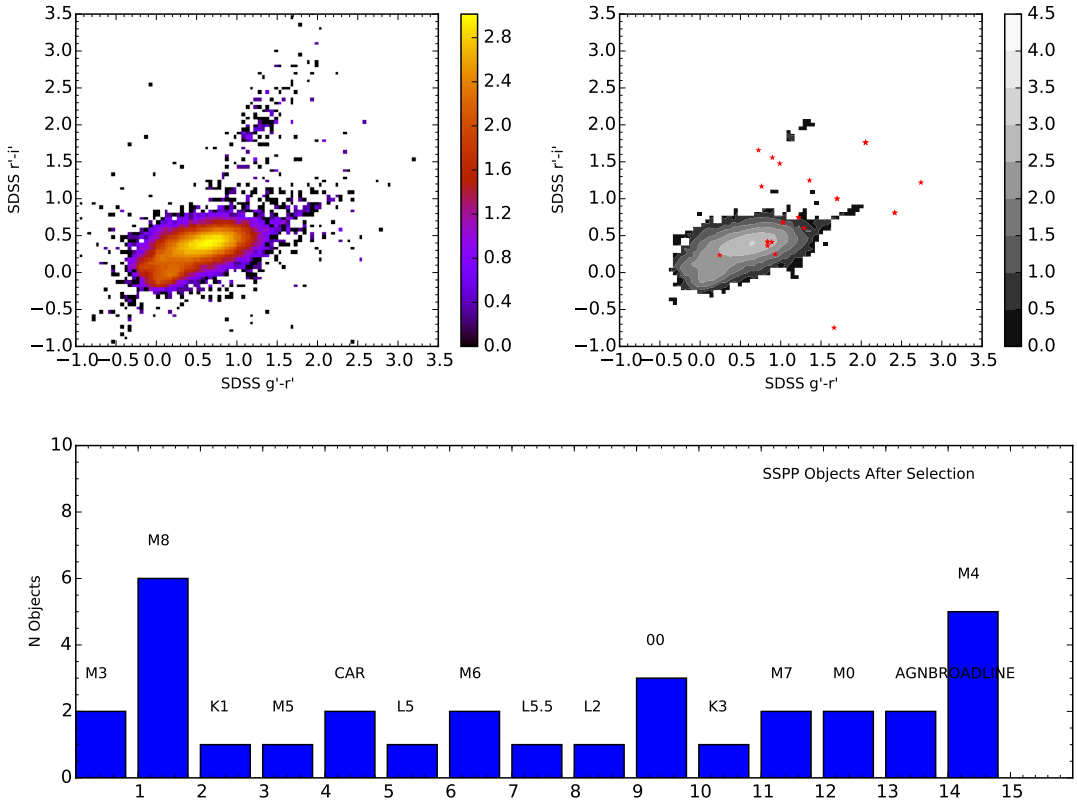

Fig. 4.— Some histogram

Ivezić, Ż., Connolly, A., VanderPlas, J., & Gray, A. 2013, Statistics, Data Mining, and Machine Learning in Astronomy

Ivezić, Ž., et al. 2000, *A. J.*, 120, 963

—. 2008, *Ap. J.*, 684, 287

Jurić, M., et al. 2008, *Ap. J.*, 673, 864

Kazin, E. A., et al. 2010, *Ap. J.*, 710, 1444

Kroupa, P. 2001, *M.N.R.A.S.*, 322, 231

Majewski, S. R. 1993, *Ann. Rev. Astr. Ap.*, 31, 575

Majewski, S. R., Skrutskie, M. F., Weinberg, M. D., & Ostheimer, J. C. 2003, *Ap. J.*, 599, 1082

Matsuura, M., et al. 2005, *Astr. Ap.*, 434, 691

Newberg, H. J., et al. 2002, *Ap. J.*, 569, 245

Table 3: Sample Selection Completeness and Contamination

Population	SIMBAD AGB*	C*	Mira	OH/IR	S*
Completeness	89.62%	72.11%	95.62%	39.53%	22.31%
Population	MACHO seq1	seq2	seq3	seq4	
Completeness	88.45%	81.08%	28.77%	14.75%	
Population	OGLE-III C-rich	O-rich	**All AGB Stars**		
Completeness	73.09%	70.68%	**79.07%**		
Population	DR12 SSPP	DR7 LRG	Galaxies	QSO	AGN
Contamination	0.56%	0.00%	0.00%	0.07%	0.00%

Olofsson, H., González Delgado, D., Kerschbaum, F., & Schöier, F. L. 2002, *Astr. Ap.*, 391, 1053

Soszyński, I., et al. 2009, *Acta Astronomica*, 59, 239

—. 2011, *Acta Astronomica*, 61, 217

Tu, X., & Wang, Z.-X. 2013, Research in Astronomy and Astrophysics, 13, 323

Udalski, A., Szymanski, M. K., Soszynski, I., & Poleski, R. 2008, *Acta Astronomica*, 58, 69

Vivas, A. K., & Zinn, R. 2006, *A. J.*, 132, 714

Vivas, A. K., et al. 2001, *Ap. J. (Letters)*, 554, L33

Wenger, M., et al. 2000, *Astr. Ap. Suppl.*, 143, 9

Wright, E. L., et al. 2010, *A. J.*, 140, 1868

Yanny, B., et al. 2000, *Ap. J.*, 540, 825

York, D. G., et al. 2000, *A. J.*, 120, 1579